Advanced pattern formation

Amplitude equations and wave fronts

Steffen Rulands

Cambridge, 23. 9. 2014

These are lecture notes of a tutorial held for the Theory of Living Matter group in Cambridge. To make the most out of these notes the reader should have an understanding of the fundamentals of non linear dynamics and the theory of pattern formation, in particular linear stability analysis.

Contents

Introduction

Life is an ongoing struggle for order. While the second law of thermodynamics predicts that in any closed system the degree of disorder increases with time, biological systems exhibit a great amount of organization. Indeed, functional differentiation of the organism's internal structure is a necessity for the development of life. Such functional differentiation is established through the formation of complex patterns. As an example, eukaryotic cells are complex organisms which are, in part, organized by smaller subunits, the organelles. On the level of tissues, the establishment of spatial order is one of the most important tasks in embryonic development. Starting from a homogeneous cluster, cells differentiate to a variety of different forms of tissue. But how can cells which share identical genetic information develop into the correct cell types in order to build functioning organisms?

To understand the formation of spatial patterns mathematical models combining nonlinear reactions and diffusion have been extensively studied. In his visionary work, Alan Turing investigated the stability of the simplest possible reaction-diffusion system which is capable of forming a pattern from a uniform state. In this lecture I will give an introduction some to advanced topics in pattern formation. The first part of this lecture deals with amplitude equations, which then naturally motivate the study of travelling wave fronts. The second part of this lecture therefore concerns wave propagation phenomena, in particular waves propagating into unstable and metastable states.

1 Amplitude equations

In linear stability analysis we linearized around a homogeneous, unstable state, $\mathbf{u}^-$; we then studied the rate $\sigma(q)$ of exponential growth or decay of perturbations with a given wave number q. When tuning some parameter ϵ the homogeneous state becomes marginally unstable.

How the growth rate σ behaves near the onset of an instability defines the class a specific instability belongs to. For example, if the maximum of σ is located at a finite wave number for all values of ϵ the instability is termed a type-I instability. If, on the other hand, the maximum of σ corresponds to a homogeneous system ($q = 0$) for $\epsilon < 0$, while the maximum of σ is located at a finite wave length for $\epsilon > 0$ the instability is termed a type-II instability. Lastly, in type-III instabilities homogeneous perturbations maximise σ for all values of ϵ. For all types of instabilities the maximum growth rate at onset can be real, corresponding to stationary patterns (s), or complex, leading to temporal oscillations (o). For simplicity, we here focus on type-I-s instabilities.

In linear stability analysis, the pattern resulting from a perturbation of the unstable state is associated with the critical wave number, q_c, which is the first wave number to grow upon onset of the instability. However, in realistic cases, the system is not tuned to be precisely at the onset of the instability but beyond, such that a finite interval of wave numbers grow exponentially in the linear regime [Figure 1(a)]. How is the exponential growth saturated? Which of the wave numbers

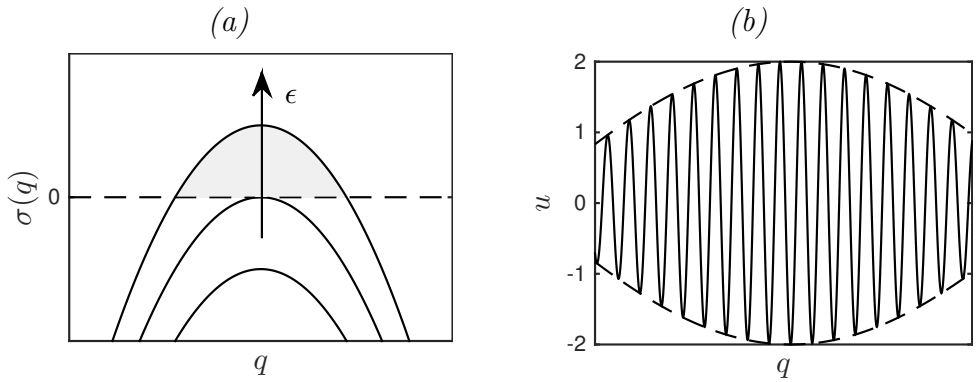

Figure 1: (a) Beyond the onset of an instability many fourier modes grow exponentially (shaded region). (b) The superposition of oscillators with similar frequency leads to a slow beating in the overall amplitude.

is actually selected for pattern formation? To answer these questions we have to take into account the non linear terms in the evolution equations describing the pattern forming system. This is investigated in the *amplitude equation formalism*. The general idea is that, near onset, the time evolution of the many fields that describe a biological system (e.g. the concentration of different transcription factors) can be effectively captured by the evolution of a single, complex-value field $A(x,t)$ - called *amplitude*. The evolution equation of $A(x,t)$ is called *amplitude equation*.

To understand the meaning of the amplitude note that near onset a constrained range of *similar* wave number is accelerated by the dynamics. The resulting oscillation can be illustrated by the superposition of two oscillators with almost equal frequencies,

$$\cos(q_1 x) + \cos(q_2 x) = 2\cos\left(\Delta q\, x/2\right)\cos\left(q_c x\right)\ , \tag{1}$$

with $\Delta q = q_2 - q_1$ and $q_c = (q_1 + q_2)/2$. For this example we hence find an oscillation with the average wave number of the single oscillators,

whose amplitude varies slowly with a wave number given by their difference. The superposition of oscillations with similar frequencies therefore leads to a "beating" in the overall amplitude. For a pattern forming system exhibiting a type-I-s instability this means that the strength of the pattern (the amplitude) varies much more slowly than the pattern itself, cf. Figure 1(a).

To derive the amplitude equation we therefore make the ansatz that a stationary pattern with wave number q_c (maximising the growth rate σ) is modulated by a slowly varying, complex amplitude,

$$\mathbf{u}(x,t) = \mathbf{u}^- + \underbrace{A(x,t)}_{\text{Amplitude}} \underbrace{\mathbf{u}_0\, e^{iq_c x}}_{\substack{\text{stationary pattern}\\ \text{with critical}\\ \text{wave number}}} + \underbrace{A(x,t)^* \mathbf{u}_0\, e^{-iq_c x}}_{\text{complex conjugate}} + \dots\,, \quad (2)$$

where $\mathbf{u}^-$ is the unstable base state. This ansatz is sensible for type-I-s instabilities. To illustrate the meaning of the complex amplitude we write it in the form $A(x,t) = a(x,t)e^{i\varphi(x,t)}$. Here, the real amplitude $a(x,t)$ gives the overall strength of the pattern. The complex phase leads to a spatio-temporal distortion of the ideal pattern, and thereby, importantly, it captures information about symmetries in the pattern. To derive the evolution equation of $A(x,t)$ one could in principle substitute this ansatz into the partial differential equations describing the time evolution of the biological system. One can, however, derive the amplitude equation by *symmetry arguments*. Similarly to the derivation of a Ginzburg-Landau theory in statistical physics we take into account the simplest terms, which are in agreement with certain fundamental symmetries of the system:

1. The amplitude equation should be invariant under translation

of the pattern by a multiple of the critical wavelength of the pattern, $A \to Ae^{i\Delta}$ (translation symmetry). To see this we substitute this transformation into the ansatz,

$$\mathbf{u}(x,t) = A(x,t)e^{i\varphi(x,t)}\mathbf{u}_0 e^{iq_c x} + A(x,t)^* e^{-i\varphi(x,t)}\mathbf{u}_0 e^{-iq_c x} \quad (3)$$

$$= A(x,t)\mathbf{u}_0 e^{iq_c(x+\Delta/q_c)} + A^*(x,t)\mathbf{u}_0 e^{-iq_c(x+\Delta/q_c)}\,. \quad (4)$$

2. The amplitude equation should also remain unchanged upon inversion of the spatial coordinates, i.e. complex conjugation $A \to A^*$ and then $x \to -x$ (parity symmetry)

While we here focus on a single extended coordinate, in two spatial dimensions we would also require the system to be isotropic, i.e. to be invariant under rotation.

With these symmetries defined we can now construct an evolution equation for $A(x,t)$. To this end we take into account the lowest order terms, which are invariant under these symmetry transformations. The simplest time derivative consistent with these symmetries is $\tau_0\partial_t A$, which defines the left hand side of the amplitude equation. A first derivative in time is also what we expect from a driven dissipative system. The right hand side potentially involves integer powers of A, A^*, or combinations of both, but also spatial derivatives as well as mixed terms. First note that any even power of A is not consistent with the symmetries, e.g. $A^2 \to A^2 e^{i2\Delta}$. This also holds true for some odd powers, which can easily confirmed by simple calculations. On the other hand, odd powers of A and its complex conjugate A^* are all invariant under the symmetry conditions. The simplest terms not involving derivatives that lead to growth and saturation are therefore

are ϵA and $g_0|A|^2A = g_0A^*A^2$.

Also, while first order derivatives are invariant under the symmetries we can rescale the amplitude A to eliminate them from the amplitude equation. The lowest order derivative to appear in the amplitude equation therefore is the second derivative, $\xi_0^2\partial_{xx}A$.

Taken together we find

$$\partial_t\tau_0 A(x,t) = \epsilon A(x,t) - g_0|A(x,t)|^2A(x,t) + \xi_0^2\partial_{xx}A(x,t)\,. \tag{5}$$

This is the amplitude equation for a type-I-s instability. Higher order terms are neglected as near onset $A(x,t)$ varies slowly in space and time, which can be formalised by a multiple scales analysis. Since the amplitude equation is therefore effectively derived as an expansion in the small parameter ϵ, this also limits the validity of the amplitude equation to slow distortions of ideal patterns near onset.

The parameters τ_0, ξ_0, and g_0 are constants that depend on the details of the biological system and must be calculated from the full evolution equations of the dynamics. While these parameters must be known in order to quantitatively describe pattern forming systems the shape of the amplitude equation does not depend on these details. Indeed, we can eliminate the physical constants by rescaling time, space, and the amplitude. We set

$$\tilde{A} = \sqrt{g_0}A\,, \quad \tilde{x} = x/\xi_0\,, \quad \tilde{t} = t/\tau_0\,, \tag{6}$$

such that the amplitude equation obtains the dimensionless form

$$\partial_t\tilde{A}(x,t) = \epsilon\tilde{A}(x,t) - |A(x,t)|^2\tilde{A}(x,t) + \partial_{xx}\tilde{A}(x,t)\,. \tag{7}$$

We can even eliminate the remaining parameter ϵ by substituting

$$\tilde{A} = \sqrt{\left|\frac{g_0}{\epsilon}\right|} A\,, \quad \tilde{x} = \frac{\sqrt{|\epsilon|}}{\xi_0} x\,, \quad \tilde{t} = \frac{\epsilon}{\tau_0} t\,. \tag{8}$$

With this, the amplitude equation obtains the parameter-free form

$$\partial_t \tilde{A}(x,t) = \pm \tilde{A}(x,t) - |\tilde{A}(x,t)|^2 \tilde{A}(x,t) + \partial_{xx} \tilde{A}(x,t)\,, \tag{9}$$

where the sign in the linear term is positive if $\epsilon > 0$ and negative if $\epsilon < 0$. Despite the limited range of validity of the amplitude equation, its importance arises from the fact that it does not depend on the microscopic details of the pattern forming system. Rather, it only depends on the *universality class* of the instability. In other words, near the onset of an instability the form of the amplitude equation only depends on symmetries, i.e. on the type of instability. Therefore, near onset, the formation of spatio-temporal patterns is similar for all systems which belong a given universality class. For example, all one dimensional patterns with a finite wavelength pattern behave similarly according to Eq. (9).

The dimensionless form of the amplitude equation not only tells us something about the universality of pattern forming processes. The absence of the small parameter ϵ in the rescaled amplitude equations (9) immediately suggests the scaling behavior ofWe may also infer the scaling behavior of the time and length scales, and the amplitude near onset. The typical time scale of the dynamics is given by τ_0/ϵ, which diverges near onset. In other words, the time evolution of the amplitude slows down near onset. The same holds true for the typical length scale, which is $\xi_0/\sqrt{\epsilon}$. On the other hand, the amplitude scales

with $\sqrt{\epsilon}$, such that the intensity of the pattern grows linearly as we approach onset.

Literature

1. M. C. Cross and H. Greenside, *Pattern Formation and Dynamics in Nonequilibrium Systems*, Cambridge University Press, Cambridge (2009)
2. M. C. Cross and P. C. Hohenberg, *Pattern formation outside of equilibrium*, Reviews of Modern Physics **65**, 851 (1993)

2 Fronts

Until now we looked at Fourier mode perturbations that were delocalised over the whole system. In reality, perturbations are constrained to a finite region. Such a local perturbtion may then saturate before spreading through the system. As the result one observes the propagation of an interface with a stationary profile - a *wave front*. We are therefore interested in front solutions of the amplitude equation. For simplicity, we focus on real solutions u, which arise from real valued perturbations. Consider equations of the form

$$\partial_t u = f(u) + \partial_{xx} u \,, \tag{10}$$

We are looking for solutions connecting the saturated state u_s with the base state u_0, and make a travelling wave ansatz,

$$u(x,t) = U(\xi), \text{ with } \xi = x - ct \,, \tag{11}$$

and the boundary conditions $u(\xi \to -\infty) \to u_s$ and $u(\xi \to \infty) \to u_0$. Substituting this ansatz into the reaction-diffusion equation (10) we obtain an ordinary differential equation for the stationary profile in the co-moving frame, U,

$$\underbrace{U''}_{\text{mass } 1} + \underbrace{c\,U'}_{\text{friction } c} + \underbrace{f(U)}_{\text{potential } \partial_U V} = 0 \,. \tag{12}$$

What is the velocity of the propagating wave front? The possible values of c are defined by the solvability of this differential equation. While this leads, in general, to an eigenvalue problem involving a

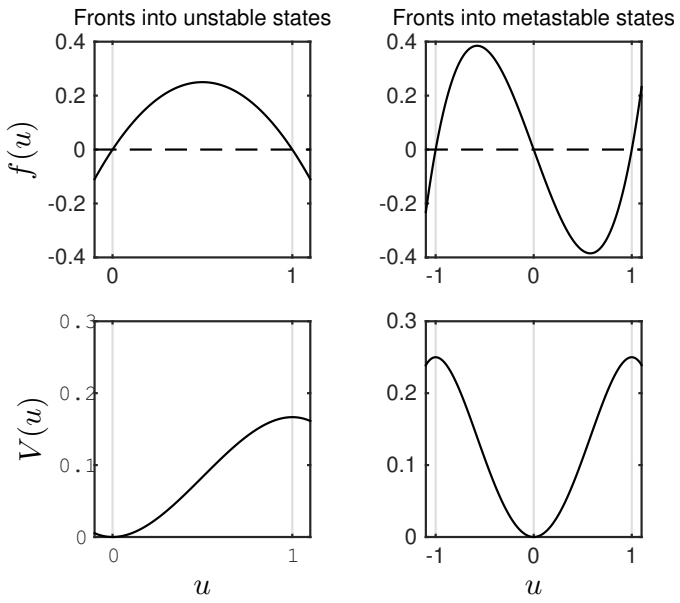

Figure 2: Reaction terms (top row) and potentials (bottom row) for two classes of propagating wave fronts: front propagating into unstable states (left column) and front propagating into metastable states (right column).

complicated, non linear differential equation we may get some insight by noting that this equation describes a mechanical system, which we can intuitively understand. The equation describes the time evolution of the position of a ball of mass 1, which is sliding through a potential $V = \int f(U)\,\mathrm{d}U$ with a friction c. The boundary conditions on the front profile dictate that the ball initially starts at the upper fixed point, u_s, and finally has to rest on the lower fixed point u_0.

Naturally, the shape of the potential $V(U)$ defines the dynamics of the ball. We here focus on two generic classes of potentials, as depicted in Figure 2: in the first case, the reaction term $f(U)$ is zero at u_0 with $f'(U) > 0$, and it vanishes at u_1, but with $f'(U) < 0$. For homogeneous systems f therefore has an unstable fixed point at u^- and a stable fixed point at u^+. The potential therefore exhibits a well at u^-, which

is surrounded by flanks of equal height. It is intuitively clear, that a ball starting on the top of the right flank will eventually rest at u^- for any positive value of the friction c. Translated to the problem of velocity selection of propagating wave fronts this mean that there is a continuous spectrum of front solutions with different velocities that solves Eq. (10). Henceforth we refer to these solutions as *fronts propagating into unstable states*.

In the second class of models we will be interested in, the reaction term f has three roots, at u_0, u_1, and u_2, where $f'(u^-) < 0$, $f'(u^0) > 0$ and $f'(u^+) < 0$. Such reaction terms lead to bistable dynamics of the homogeneous system: a system prepared in the state u_0 will remain there exponentially long. Only a large enough perturbation will lead to excitation and an acceleration of the dynamics towards the upper stable fixed point, u^+. The potential now has two maxima, at u^- and u^+, as well as a local minimum at u^0. From the sliding ball analogy we infer that there is only a discrete value of the friction which would lead to a ball starting at u^+ to rest at u^-. We refer to the solutions of such partial differential equations as *fronts propagating into metastable states*.

It is important to note that propagating wave fronts arise in nearly all fields of science - not only as solutions of amplitude equations. For example, fronts propagating into unstable states have been used to describe range expansion processes, such as the expansion of bacterial populations of epidemic spreading. Fronts propagating into metastable states arise, for example, in ecology when populations are subject to a strong Allee effect. Both classes of propagating wave

fronts have been studied extensively in the literature. In the following, we will give a short overview on some of the concepts which play a role in both classes of wave fronts.

2.1 Front propagation into unstable states

Fronts propagating into an unstable state are an ubiquitous phenomenon in nature. They describe, for example, the spreading of advantageous genes [1] or infectous diseases [2]. Recently, they have attracted considerable attention as a model for the range expansion of bacterial populations [3–5].

As we have seen in the sliding ball analogy fronts propagating into unstable states allow, in principle, for a continuous spectrum of front solutions. From this continuous spectrum possible velocities, which one is selected by the expansion dynamics? For simplicity, we here focus on the Fisher-Kolmogorov equation,

$$\partial_t u(x,t) = \epsilon u(x,t) - u(x,t)^2 + \partial_{xx} u(x,t)\,. \tag{13}$$

It is easy to see that the reaction term comprises a stationary, homogeneous state at $u^- = 0$, which is unstable, and a stable, homogeneous state at $u^+ = 1$. Hence, small perturbations of the unstable state grow exponentially and ultimately saturate. In the context of bacterial range expansion the unstable state corresponds to an unpopulated system containing nutrients. The the stable state describes a fully occupied system, where all nutrients have been consumed for reproduction. If the unstable state is perturbed in a confined region

the saturated solution will spread through the system. In other words, we expect a wave front to propagate into the unstable state.

One of the central insights in the theory of front propagation into unstable states is that the velocity of the front is determined by its tip. This is intuitive, as in the bulk the system rests in its saturated state, while perturbations in the tip are exponentially accelerated. Since concentrations in the tip are small we may therefore start by linearizing around the unstable state and write solutions in the form

$$u(x,t) = \frac{1}{2\pi} \underbrace{\int \mathrm{d}q\, e^{iqx+\sigma(q)t}}_{\substack{\text{Propagation of IC} \\ \text{in space and time}}} \underbrace{\int dx'\, u_0(x') e^{iqx'}}_{\substack{\text{Fourier transform} \\ \text{of initial conditions}}} . \tag{14}$$

Note that the integral is only defined for sufficiently local initial conditions. We evaluate the integral at a moving point $x = vt$,

$$u(x = vt, t) = \frac{1}{2\pi} \int \mathrm{d}q\, e^{[iqv+\sigma(q)]t} \int dx'\, u_0(x') e^{iqx'} . \tag{15}$$

For large times wave numbers are rapidly varying, which leads to a decoherent superposition of wave modes, effectively cancelling out each other. The integral is therefore dominated by the region, where argument of the exponential varies most slowly, the stationary phase. This stationary determined is given by $\partial_q[iqv + \sigma(q)] = 0$, or equivalently

$$v = i \frac{\mathrm{d}\sigma}{\mathrm{d}q}\bigg|_{q=q_s} , \tag{16}$$

from which we can derive the stationary point q_s. With this, employing the stationary phase approximation, we write our ansatz as

$$u(x = vt, t) \propto e^{[iq_s v+\sigma(q_s)]t}. \tag{17}$$

If v is chosen to correspond to the velocity of the travelling wave front the profile should be stationary. Making use of this self-consistency requirement, we assume that the solution in the tip of the front neither grows nor decays exponentially, i.e. the real part of the argument vanishes, $\Re[iq_s v + \sigma(q_s)] = 0$. This yields a second equation for the front velocity,

$$v^* = \frac{\Re[\sigma(q_s)]}{\Im[q_s]}\,. \tag{18}$$

Let's look at the application of this result to the Fisher-Kolmogorov equation. The spectrum

$$\sigma(q) = \epsilon - q^2\,, \tag{19}$$

from which we obtain the equations that determine the velocity,

$$v = 2iq_s \text{ and } v = i\frac{\epsilon - q_s^2}{q_s}\,. \tag{20}$$

We first find that the stationary point is given by $q_s = i\sqrt{\epsilon}$. From this the velocity follows as

$$v^* = 2\sqrt{\epsilon}\,. \tag{21}$$

This is the *linear spreading velocity* of the front: the velocity with which small perturbations of the unstable state grow and spread according to the evolution equations obtained by linearizing the full model around the unstable state.

In our derivation of the linear spreading velocity we took the fourier transform of the initial conditions and evolved this in space and time.

In order for this ansatz to be well-defined we must assume that the initial conditions are sufficiently localized, i.e. they have compact support. In many real applications this is not the case. Remarkably, it turns out that all initial conditions which are sufficiently step, i.e. which decay faster than $\exp(\lambda^* x)$, asymptotically take the linear spreading velocity v^*.

Indeed, the significance of the linear spreading velocity goes far beyond the propagation speed of Fisher waves. For any front propagating into an unstable state, it is intuitively clear that stable wave solution must propagate faster than the linear spreading of small perturbations, $v \geq v^*$.

The linear spreading velocity therefore provides a unifying concept for a large variety of fronts: If $v = v^*$, as in the example of the Fisher-Kolmogorov equation, the front is termed a *pulled front*. The propagation speed of pulled fronts is determined by the leading edge of the front, such that the front is being "pulled along" by its tip. The velocity of the leading edge, as obtained by linearizing the evolution equations, therefore defines the speed of the front. Contrarily, fronts whoose velocity is larger than the linear spreading velocity, $v > v^*$ are called *pushed fronts*. For pushed fronts nonlinear terms influence the front's velocity and one might think these fronts are being pushed by nonlinear terms in the bulk region behind the front.

2.2 Front propagation into metastable states

Bistable systems are ubiquitous in nature. For example, genetic switches are bistable systems that store the activation state of a gene [6, 7]. On the other hand, in population dynamics, a minimum population size is often needed to establish a stable population. In this case one says that the population is subject to a strong Allee effect [8].

While in Turing's simple model the locally stable state looses its stability due to diffusive transport, we are here interested in how pattern formation is possible if the stable state is globally stable to small perturbations. Such systems are commonly called *excitable media* and they arise in a variety of fundamental problems in biology, chemistry, physiology and medicine [9]. As we will see, excitable media may admit the propagation of waves. These waves are paramount for some of the most fundamental processes in living organisms [9]: Excitable electrical waves are used by some single cell organisms such as *Paramecium* to control the mechanical rotation of their cilia, allowing them to adjust their swimming motions. Such excitable electrical waves also prevent multiple sperm cells from merging with an egg. When a first sperm has entered the egg an excitable wave triggers a rapid change in the egg's membrane preventing other sperms from entering.

2.2.1 Front propagating into metastable states in homogeneous environments

What can we infer about the solutions of Eq. (10) if the reaction term is bistable? If the potential $V(u) = \int f(u)\mathrm{d}u$ has two local maxima at concentrations u^- and u^+, separated by a minimum, i.e. the reaction term is bistable, solutions are stationary profiles moving with a constant velocity c,

$$u(x,t) = U(\xi),\ \xi = x - ct\,, \tag{22}$$

with $U(\xi \to \pm\infty) \to u^{\pm}$. The shape $U(\xi)$ of the front profile can be obtained by solving the stationary differential equation, $\partial_{xx}U + \partial_U V(U) = 0$. Such solutions are called *traveling wave solutions* and, as discussed above, they allow us to formulate Eq. (10) in terms of an ordinary differential equation, namely

$$U'' + cU' + \partial_U V(U) = 0\,. \tag{23}$$

Here, the prime denotes derivatives with respect to ξ. Equation (23) can be interpreted in terms of an analogous mechanical problem: it may be interpreted as a force balance equation for a particle (sliding ball) with mass 1, friction c and potential $V(\phi)$. The boundary conditions are determined by the asymptotic values $u^{\pm}$ of the front profile, i.e. the ball starts at one maximum and ends at the other maximum. To determine the front's velocity we have to solve the Eigenvalue problem defined by Eq. (23). In the language of the sliding ball analogy, this problem can be formulated as follows: for which friction c does the ball, when starting at the maximum u^+ at high concentrations, stop exactly at the maximum u^- at low concentrations? If the

friction is positive, solutions are traveling waves propagating in the positive x direction. On the other hand, if the friction is negative, the front propagates into the negative x direction.

To derive an expression for the front's velocity we multiply Eq. (23) with ϕ' and integrate over ξ. We obtain

$$\int_{-\infty}^{\infty} f(U)\frac{\mathrm{d}U}{\mathrm{d}\xi}\mathrm{d}\xi + \int_{-\infty}^{\infty} U''U'\mathrm{d}\xi + c\int_{-\infty}^{\infty}(U')^2\mathrm{d}\xi = 0\,. \tag{24}$$

From the asymptotic values of the front solution, $U(\pm\infty) = u^{\pm}$ we find that the first term on the left hand side equals $-\int_{u^-}^{u^+} f(U)\mathrm{d}U \equiv -\Delta V$. The second integral on the left hand side vanishes, as one may see by employing the substitution law. We obtain an expression for the front's velocity,

$$c = \frac{\Delta V}{\int_{-\infty}^{\infty}(U')^2\mathrm{d}\xi}\,. \tag{25}$$

Therefore, two factors determine the speed of the propagating wave front: the difference in potential between the stable states gives the direction of propagation and the absolute value of the velocity. If ΔV is positive, the front propagates into the positive x-direction and vice versa for negative values of ΔV. The denominator can be thought of as a measure for the maximum steepness of the front. We infer that steep fronts move slower than shallow fronts.

2.2.2 Front propagation into metastable states in inhomogeneous environments

Turing's mechanism has long been thought to be active in early developmental processes, such as the segmentation of embryos. However, it turned out that this is not the case. Indeed, Turing patterns are translationally invariant, which is not a desirable property if one want to define precisely located patterns. In principle, the stripe patterns arising through Turing's mechanism could be positioned through appropriate boundaries, but then it is unclear what happens if the wavelength of these patterns is of the order of the system size, as in early development.

During the development of an embryo cells differentiate into a variety of distinct cell types, such as nerve cells, phosphoreceptor cells of the retina in the eye, or muscle cells. How form and patterns emerge from a homogeneous cluster of cells has already fascinated Aristotle in the fourth century B.C.. He described the multiple forms of morphogenesis in birds, plants and cephalopods, already noting that an animal's egg contained the "potential" for its later differentiation. In 1969, Lewis Wolpert was the first to propose that asymmetric concentrations of a chemical signal (morphogens) provide positional information for the developmental system [10]. The positional signal serves as an input to the gene regulatory system allowing the cell or nucleus to differentiate accordingly.

An important example arises in the early embryogenesis of *Drosophila melanogaster* where maternal morphogen gradients provide positional information for downstream gene regulatory processes [11–14]. The

morphogen Bicoid is translated from RNA which is located at the anterior end of the egg. The combined effect of this source, degradation and diffusion leads to an exponentially decreasing concentration of Bicoid. This gradient defines an anterior-posterior axis, thereby providing positional information to processes determining cell differentiation.

The first gene activated by Bicoid is called Hunchback, which is expressed at the anterior end of the embryo. Importantly, it exhibits a sharp on-off boundary changing from its largest to its lowest concentration in only one tenth of the egg's length along the anterior-posterior axis [Fig. 3(b)]. Experimental studies have shown that the production of Hunchback is governed by cooperative self-activation and cooperative activation by Bicoid [13, 15–17]. As Hunchback again serves as a positional signal for downstream developmental processes, such as the formation of the gap genes giant, krüppel and knirps, the exact position of the Hunchback front is pivotal to the embryo's fate [13]. Hence, the boundary's stability to extrinsic perturbations or internal noise is paramount.

Spatially inhomogeneous activation is also relevant in other contexts. In ecology, birth rates may have spatial dependence, *e.g.* due to spatial variance in temperature or resource availability [18, 19]. In cell biology, bistability and spatially inhomogenous activation has been proposed as a mechanism responsible for the polarization of cells [20–22].

Motivated by these processes, we will in the following extend the methodology developed in the previous section to situations, where waves propagating into metastable states are subject to spatially

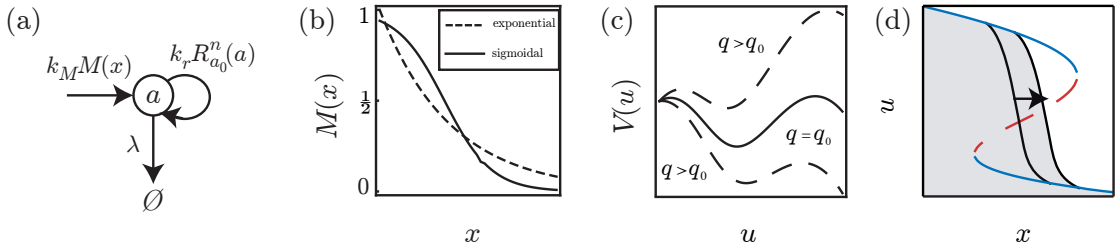

Figure 3: (a) The model comprises self-activation with a rate depending nonlinearly on the concentration a, degradation and activation by an external positional signal $M(x)$. (b) Two types of gradients: exponential decay (dashed line) and a sigmoidal profile ensuing from regulating an exponentially decaying input (solid line). (c) The potential for different values of the front position q. The sliding ball analogy states that the front localizes where the two maximum values of the potential are equal. (d) Sketch of the bifurcation diagram and traveling wave solution of Eq. (10). Blue lines denote stable solutions while the dashed (red) line corresponds to the unstable branch. Wave fronts (black lines and shaded area) penetrating the bistable region slow down and eventually come to rest at a stable fixed point of the front dynamics.

varying influences. To this end, we will investigate a broad class of bistable diffusion-reaction models with reaction terms comprising self-activation, external activation, and degradation. While self-activation and degradation are assumed to be spatially uniform, the external activation is taken to be position-dependent.

While we will employ a model framework, which is inspired by early Drosophila embryogenesis it is important to note that we should not expect such a model to give quantitatively correct descriptions of real biological systems. Indeed, the details of gene regulatory networks in embryogenesis are not fully understood, even today. A quantitative analysis of a model comprising many parameters is therefore not always the best strategy. Therefore, we will study the simplest model

allowing for the stable establishment of a sharp boundary. In the context of embryogenesis it can be thought of as a coarse grained biochemical network, which despite being simple comprises essential characteristics of the more complex networks found in biology. Specifically, we consider a one-dimensional system where diffusing particles are subject to three types of reactions: First, there are gain processes with a concentration-dependent rate that accounts for self-activation in gene regulatory systems or reproduction in population dynamics. Typically, these rates are small for low concentrations, then rise and finally saturate at high concentrations. In populations dynamics, this behavior is referred to as the strong Allee effect [8, 24]. In gene regulation, it can be due to cooperative transcription factor binding to a gene promoter. A common choice for the overall reaction rate is $k_r R^n_{a_0}(a)$ with the *Hill function*

$$R^n_{a_0}(a) \equiv a^n/(a_0^n + a^n) \ , \tag{26}$$

k_r the maximum intrinsic production rate, and a the particle concentration. The Hill coefficient n measures the degree of cooperative binding in the promoter region, or, in ecology, the strength of an Allee effect. Second, we account for loss processes, where particles vanish with a certain rate λ. Third, in addition to self-activation, there may also be external sources for particle production. Here, we are interested in systems where this source is position-dependent and characterized by the overall rate $k_M M(x)$. The prefactor k_M denotes the maximum rate of external activation, and $M(x)$ is a monotonically decreasing positive density profile with normalization $M(0) = 1$. In the simplest case, where the profile results from a source-degradation dynamics [25, 26], it is exponential $M(x) = e^{-x/\xi}$

with the decay length ξ, cf. Fig. 3 (a). Prominent examples are the concentration profile of Bicoid in *Drosophila* [25] and temperature or nutrient gradients in population dynamics [27]. Since the production of Hunchback by Bicoid is mediated by cooperative binding, the profile $M(x)$ entering the overall production rate is commonly described by $M(x) \sim R^m_{I_0}(e^{-x/\xi})$ [15]. The exponentially decaying signal induced by maternal source-degradation dynamics serves as an input to the gene regulation system. The latter is described by a Hill coefficient m typically in the range from 1 to 5, and an activation threshold I_0. The model is summarized in Fig. 3(a).

In the limit of a large system size, fluctuations are of minor importance and the spatio-temporal dynamics is then aptly described by a reaction-diffusion equation, which in dimensionless form reads

$$\partial_t u = f(u, x) + \partial_{xx} u \,. \tag{27}$$

Here,

$$f(u, x) \equiv r R^n_{u_0}(u) + M(x) - u \tag{28}$$

comprises self-activation, external activation and degradation. Concentration u, time t, and space x are measured in units of k_M/λ, $1/\lambda$ and $\sqrt{D/\lambda}$, respectively. The ratio $r \equiv k_r/k_M$ denotes the relative amplitude of self-activation and external activation mediated through $M(x)$.

Sliding ball analogy for inhomogeneous systems Traveling wave solutions of Eq. (10) may be localized due to the combined effect of spatially varying external sources and bistability [21, 22, 28]. The

basic mechanism can be best understood in terms of the well-known sliding ball analogy [9], which here is complicated by the fact that the reaction term is space-dependent. Since in most biological situations a steep profile in u is induced by a smooth external profile $M(x)$, we may assume a separation of length scales $\xi \gg \sqrt{D/\lambda}$ and ξ much smaller than the system size. Then one can make a generalized traveling wave ansatz

$$u(x,t) = U(x - q(t), y), \tag{29}$$

where x is a fast varying variable describing changes in the concentration profile, $y = x/\xi$ is a slowly varying variable describing changes in the external profile $M(x)$, and $q(t)$ denotes the front position. Substituting the generalized traveling wave ansatz into Eq. (27) we obtain to leading order in the inverse length of the external gradient,

$$-\dot{q}\partial_x U = \partial_{xx} U + \partial_U V(U, y) + \mathcal{O}(\xi^{-1})\,. \tag{30}$$

This differential equation may be interpreted as a force balance for a particle (sliding ball) with mass 1, friction $\dot{q}$ and potential $V(u,y) = \int^u f(\tilde{u}, y)\mathrm{d}\tilde{u}$. Importantly, the potential parametrically depends on y, see Figure 3(b). For parameter regimes where V has two maxima at $u^+(x)$ and $u^-(x)$, and a local minimum at $u^s(x)$, the velocity $\dot{q}$ must be chosen such that the sliding ball starting from the upper branch u^+ ends up at the lower branch u^-. The front speed is proportional to the difference between the two maxima of $V(u,y)$ and becomes zero if the Maxwell condition

$$\Delta V(y) \equiv \int_{u^-}^{u^+} f(u,y)\mathrm{d}u = 0 \tag{31}$$

is satisfied. More quantitatively, in analogy to the homogeneous case [9, 29, 30], one finds

$$\dot{q} \approx \frac{\Delta V(q)}{\int_{-\infty}^{\infty}[\partial_x U(x-q,y)]^2 \mathrm{d}x} \equiv c(q)\,, \tag{32}$$

where $U(x-q,y)$ is the traveling wave solution. The denominator roughly equals the maximum steepness of the front profile, and implies that steep fronts move slower along the gradient [9]. One may also arrive at this equation employing a variational ansatz called *Whitham principle* [29, 30]. With Eq. (32) we have transferred the partial differential equation, Eq. (10), to an ordinary differential equation describing the time evolution of the front positions. We can now employ the standard methods of non linear dynamics to calculate the dynamics of the front profile in an inhomogeneous environment defined by M.

Derivation of the localization position The above analysis shows that the velocity of the wave front is proportional to the potential difference between the stable states. As this potential explicitly depends on the position of the front it is natural to ask whether there is any position q_0 where the potential difference, and thereby the velocity, vanishes. For simplicity we here focus on monotonically decreasing activating gradients $M(x)$. Equation (27) admits traveling waves solutions if the potential $V(u,x) = \int^u \mathrm{d}\tilde{u}\, f(\tilde{u},x)$ exists locally. In our case we can analytically perform the integral and obtain

$$V(u,x) = -u\left[\frac{u}{2} - M(x) - r + F\left(\frac{u^n}{u_0^n}\right)\right], \tag{33}$$

where $F(z) \equiv {}_2F_1(1, 1/n, 1+1/n, -z)$ and ${}_2F_1$ is the Gauss hypergeometric function. The wave localizes if the difference in the maximum values of the potential is zero, $\Delta V(q_0) = 0$.

To proceed, we need to know the location of the stable points as a function of $M(x)$. In our class of models, a single branch of stable solutions at high concentrations typically undergoes a fold bifurcation for decreasing concentrations of the morphogen $M(x)$ (growing x), where the system is bistable on a confined spatial interval, see Figure 3 (d). For low values of $M(x)$ (large x), a single branch at low concentrations remains. Within the bistable regime, the velocity $c(q)$ may change sign and thereby lead to a localization of the traveling wave front. We next calculate the concentrations corresponding to the stable states by finding the roots of the reaction term $f(u, x)$. For the lower stable state, u^-, we expand the Hill function in the reaction term about $u = 0$ in powers of u,

$$R^n_{u_0}(u) = \sum_{k=1}^{\infty} (-1)^{k+1} \left(\frac{u}{u_0}\right)^{kn} , \tag{34}$$

i.e. for low concentrations the first nonlinear term is of order u^n. For large concentrations, we expand the Hill function as a Laurent series, obtaining

$$R^n_{u_0}(u) = 1 - \sum_{k=1}^{\infty} (-1)^{k} \left(\frac{u}{u_0}\right)^{-kn} , \tag{35}$$

such that the first non linear correction is of order u^{-n}. To calculate the stable states we therefore linearize $f(u, x)$ in u and find

$$u^+(x) \approx M(x) + r \text{ and } u^-(x) \approx M(x) . \tag{36}$$

With this, we are now in a position to give an approximate expression

for the difference between the two maximum values of the potential,

$$\Delta V(q) = V(u^+(q)) - V(u^-(q)) \tag{37a}$$

$$= \frac{r}{2}\left[r + 2M(q)F\left(\frac{M(q)^n}{u_0^n}\right) - 2\big(M(q)+r\big)F\left(\frac{(M(q)+r)^n}{u_0^n}\right)\right]. \tag{37b}$$

As ΔV is to a good approximation linear in $M(x)$ we linearize around $M(x) = 0$,

$$\Delta V(x) \approx \frac{1}{2}r\left\{r + M(x)\left[2 - \frac{2}{1+\left(\frac{r}{u_0}\right)^n}\right] - 2rF\left(\frac{r^n}{u_0^n}\right)\right\}. \tag{38}$$

The localization position q_0 is then determined by $\Delta V(q_0) = 0$. Solving this equation for the concentration of the external source at which the front localizes, $M(q_0)$, we find

$$M_0 \equiv M(q_0) \approx \frac{1}{2}r\left[1 + \left(\frac{r}{u_0}\right)^n\right]\left(\frac{u_0}{r}\right)^n\left[2F\left(\frac{r^n}{u_0^n}\right) - 1\right]. \tag{39}$$

To obtain an intuitive understanding of the expression for the front position M_0 we investigate the dependence of M_0 on the parameters r and u_0. To this end, we first take the derivative with respect to r,

$$\partial_r M_0 = \frac{1}{2}\left(\frac{u_0}{r}\right)^n\left[1 + n - \left(\frac{r}{u_0}\right)^n - 2nF\left(\frac{r^n}{u_0^n}\right)\right]. \tag{40}$$

In bistable systems the relative amplitude of self-activation r is typically greater than the activation threshold u_0. Noting that $F(z) \sim 1/z$ for $z \to \infty$ we get $\partial_r M_0 \approx 1/2$, proving that M_0 is linear in r. On

the other hand, taking the derivative with respect to u_0 we get

$$\begin{aligned} \partial_{u_0} M_0 &= \frac{1}{2}\left(\frac{u_0}{r}\right)^{n-1}\left\{2\left[1+n+\left(\frac{r}{u_0}\right)^n\right]F\left(\frac{r^n}{u_0^n}\right)-2-n\right\} \\ &\approx \frac{1}{2}\left(\frac{u_0}{r}\right)^{n-1}\cdot 2\left(\frac{r}{u_0}\right)^n\cdot\left(\frac{u_0}{r}\right) \\ &= 1\,, \end{aligned} \tag{41}$$

which proves that M_0 is also linear in u_0. Note that although the arguments above strictly hold in the limit $n \to \infty$ we numerically found that they are valid even for relatively small values of n. In conclusion, we showed that M_0 can be approximated by a linear function of the form

$$M_0 \approx g(n)\cdot(u_0 - r/2)\;, \tag{42}$$

where the pre factor $g(n)$ only depends on n. By taking the limit $n \to \infty$ first, and then doing the above calculations we find that $g(n) \to 1$ for $n \to \infty$.

Stability with respect to extrinsic perturbations We now know that there is concentration M_0 where the velocity of the front vanishes. But does the front really localize at this position? To answer this question we are now interested in the stability of the fixed point q_0 of the differential equation 32. Only if this fixed point is stable the front dynamics will be attracted towards this position. In the following, we therefore perform a linear stability analysis around q_0, i.e. we investigate how the front reacts to extrinsic perturbations. How a localised front reacts to perturbations is also highly relevant for real biological systems: for example, to ensure robust embryonic develop-

ment the established segment boundaries should not be susceptible to changes in the environmental conditions.

To be stable against extrinsic perturbations the front should both relax back quickly into its equilibrium position and be insensitive to perturbations in the driving signal $M(x)$. Since a high relaxation rate implies that a front can follow changes in the signal quickly, the two stability criteria seem to be somewhat at odds. However, as shown below, they are in full accordance with the latter being less restrictive.

The relaxation rate of the front back into its equilibrium position q_0 can be assessed within the framework of a linear stability analysis [31]. Mathematically, the relaxation rate is obtained by expanding Eq. (32) at q_0:

$$c(q) = -\sigma(q - q_0) + \mathcal{O}(q - q_0)^2\,, \tag{43}$$

where $\sigma \equiv -\,\partial_q c(q)\big|_{q=q_0}$. The quantity σ measures the stability of the fixed point q_0, such that large values of σ correspond to a stably localized front. Taking the derivative of Eq. (32) with respect to the position q we find

$$\sigma = -\frac{\partial_{M(q)}\Delta V(M(q))\,\cdot\partial_q M(q)}{\int_{-\infty}^{\infty}[\partial_x U(x-q)]^2 \mathrm{d}x}\bigg|_{q=q_0} \tag{44}$$

revealing that extrinsic stability is determined by three factors: In the numerator, the first factor describes how sensitively the potential difference of the stable states depends on the external source. The second factor, $\mu \equiv |\partial M(q)/\partial q|_{q_0}$, gives the steepness of the external profile at the localization position. While, therefore, a steeper source

profile enhances front stability, the steepness of the front profile, given by the denominator, has the opposite effect. The reason simply is that according to Eq. (32), steeper fronts move slower and therefore also relax back more slowly.

For monotonically decreasing external activation $\partial_q M(q)$ is always negative, while the denominator of Eq. (44) can only be positive. According to Eq. (38), $\partial_{M(q)}\Delta V(M(q))$ is positive, such that the stability σ of the localized front is also positive. We therefore find that the wave front stably localizes at a position q_0 determined by the expression level M_0 of the activating morphogen.

One can also more quantitatively derive the stability of the localised wave front by making an ansatz for the stationary solution of Eq. (10). By making use of the approximate expressions for the stable states, $u^+(x)$ and $u^-(x)$ we assume a connection of the stable states as shown in Fig. 3(d),

$$U(x-q) = M(x) + r \begin{cases} 1 - \frac{1}{2}e^{x-q} & (x < q) \\ \frac{1}{2}e^{-(x-q)} & (x \geq q) \end{cases} , \tag{45}$$

which is a good approximation when n is not too small. Indeed, using $M(q_0) \approx u_0 - r/2$ we find that $u^n/(u_0^n + u^n)$ evaluates to 1 for $q < q_0$ and 0 for $q > q_0$. Hence,

$$f(U,x) + \partial_{xx}U = \partial_{xx}M(x) \sim \xi^{-2} \approx 0\,. \tag{46}$$

This confirms that U is an approximate stationary solution of Eq. (27).

Literature

1. M. C. Cross and H. Greenside, *Pattern Formation and Dynamics in Nonequilibrium Systems*, Cambridge University Press, Cambridge (2009)

2. W. v. Sarloos, *Front propagation into unstable states*, Physics Reports **386**, 2-6 (2003)

3. S. Rulands, B. Klünder, E. Frey, *Stability of localized wave fronts in bistable systems*, Phys. Rev. Lett. **110**, 038102 (2013)

4. S. Rulands, *Heterogeneity and spatial correlations in stochastic many-particle systems. From embryogenesis to evolution.* PhD Thesis, Ludwig-Maximilians-University Munich (2013)

References

[1] R A Fisher. The Wave of Advance of Advantageous Genes. *Annals of Eugenics*, 7(355), 1937.

[2] Denis Mollison. Spatial contact models for ecological and epidemic spread. *J. Roy. Stat. Soc. B*, pages 283–326, 1977.

[3] Oskar Hallatschek, Pascal Hersen, Sharad Ramanathan, and David R Nelson. Genetic drift at expanding frontiers promotes gene segregation. *Proc. Natl. Acad. Sci. USA*, 104(50):19926–19930, 2007.

[4] O Hallatschek and D R Nelson. Gene surfing in expanding populations. *Theoretical Population Biology*, 73(1):158–170, 2008.

[5] K S Korolev, Mikkel Avlund, Oskar Hallatschek, and David R Nelson. Genetic demixing and evolution in linear stepping stone models. *Rev. Mod. Phys.*, 82(2):1691, 2010.

[6] Bruce Alberts, Alexander Johnson, Julian Lewis, Martin Raff, Keith Roberts, and Peter Walter. *Molecular Biology of the Cell*. Garland Science, New York, 4 edition, 2002.

[7] Alexander Altland, Andrej Fischer, Joachim Krug, and Ivan G Szendro. Rare Events in Population Genetics: Stochastic Tunneling in a Two-Locus Model with Recombination. *Phys. Rev. Lett.*, 106(8):88101, February 2011.

[8] P A Stephens, W J Sutherland, and R P Freckleton. What Is the Allee Effect? *Oikos*, 87(1):185–190, 1999.

[9] Micheal Cross and Henry Greenside. *Pattern formation and dynamics in nonequilibrium systems*. Cambridge University Press, New York, 2009.

[10] L. Wolpert. Positional information and the spatial pattern of cellular differentiation. *J. Theor. Biol.*, 25(1):1–47, October 1969.

[11] Wolfgang Driever and Christiane Nüsslein-Volhard. A gradient of bicoid protein in Drosophila embryos. *Cell*, 54(1):83–93, July 1988.

[12] Wolfgang Driever and Christiane Nüsslein-Volhard. The bicoid protein determines position in the Drosophila embryo in a concentration-dependent manner. *Cell*, 54(1):95–104, July 1988.

[13] F J P Lopes, F M C Vieira, D M Holloway, P M Bisch, and A V Spirov. Spatial Bistability Generates hunchback Expression Sharpness in the Drosophila Embryo. *PloS Comput. Biol.*, 4(9):e1000184, January 2008.

[14] Filipe Tostevin, Pieter Rein ten Wolde, and Martin Howard. Fundamental limits to position determination by concentration gradients. *PloS Comput. Biol.*, 3(4):e78, April 2007.

[15] D S Burz, R Rivera-Pomar, H Jäckle, and S D Hanes. Cooperative DNA-binding by Bicoid provides a mechanism for threshold-dependent gene activation in the Drosophila embryo. *EMBO J,*, 17(20):5998–6009, October 1998.

[16] Michael W Perry, Jacques P Bothma, Ryan D Luu, and Michael Levine. Precision of Hunchback Expression in the Drosophila Embryo. *Curr. Biol.*, 22(23):2247–2252, October 2012.

[17] J Treisman and C Desplan. The products of the Drosophila gap genes hunchback and Krüppel bind to the hunchback promoters. *Nature*, 341(6240):335–7, September 1989.

[18] Rory Putman and Stephen D. Wratten. *Principles Of Ecology*. University of California Press, Berkeley, 1984.

[19] Tamás Czárán. *Spatiotemporal Models of Population and Community Dynamics*. Springer, New York, 1998.

[20] William M Bement, Ann L Miller, and George von Dassow. Rho GTPase activity zones and transient contractile arrays. *BioEssays*, 28(10):983–93, October 2006.

[21] Y Mori, A Jilkine, and L Edelstein-Keshet. Wave-pinning and cell polarity from a bistable reaction-diffusion system. *Biophys. J.*, 94(9):3684–3697, January 2008.

[22] Y Mori, A Jilkine, and L Edelstein-Keshet. Asymptotic and bifurcation analysis

of wave-pinning in a reaction-diffusion model for cell polarization. *SIAM J. Appl. Math.*, 71(4):1401–1427, December 2011.

[23] A. M. Turing. The Chemical Basis of Morphogenesis. *Philos. T. Roy. Soc. B*, 237(641):37–72, August 1952.

[24] Caz M Taylor and Alan Hastings. Allee effects in biological invasions. *Ecol. Lett.*, 8(8):895–908, 2005.

[25] Oliver Grimm, Mathieu Coppey, and Eric Wieschaus. Modelling the Bicoid gradient. *Development*, 137(14):2253–2264, 2010.

[26] O Wartlick, P Mumcu, A Kicheva, T Bittig, C Seum, F Jülicher, and M González-Gaitán. Dynamics of Dpp signaling and proliferation control. *Science*, 331(6021):1154–9, March 2011.

[27] Patrick C Tobin, Stefanie L Whitmire, Derek M Johnson, Ottar N Bjø rnstad, and Andrew M Liebhold. Invasion speed is affected by geographical variation in the strength of Allee effects. *Ecol. Lett.*, 10(1):36–43, January 2007.

[28] T H Keitt, M A Lewis, and R D Holt. Allee effects, invasion pinning, and species' borders. *Am. Nat.*, 157(2):203–16, February 2001.

[29] A K Abramyan and S A Vakulenko. Nonlinear Ritz method and the motion of defects. *Teoret. Mat. Fiz.*, 155(2):202–214, 2008.

[30] S Vakulenko, Manu, J Reinitz, and O Radulescu. Size Regulation in the Segmentation of Drosophila: Interacting Interfaces between Localized Domains of Gene Expression Ensure Robust Spatial Patterning. *Phys. Rev. Lett.*, 103(16):168102, January 2009.

[31] S Wiggins. *Introduction to Applied Nonlinear Dynamical Systems and Chaos*. Springer, Berlin, 1990.